

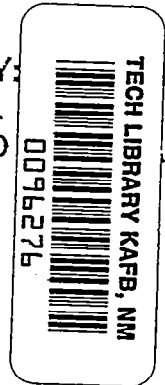
NASA MEMO 5-6-59L

~~CONFIDENTIAL~~  
UNCLASSIFIED

C. 246

# NASA

LOAN COPY:  
AFWL  
KIRTLAND



TO

## MEMORANDUM

DAMPING IN PITCH AND STATIC STABILITY OF A GROUP OF  
BLUNT-NOSE AND CONE-CYLINDER-FLARE MODELS  
AT A MACH NUMBER OF 6.83

By Herman S. Fletcher and Walter D. Wolhart

Langley Research Center  
Langley Field, Va.

**TECHNICAL LIBRARY  
KIRTLAND AFB, NM**

CLASSIFIED DOCUMENT - TITLE UNCLASSIFIED

This material contains information affecting the National Defense of the United States within the meaning of the espionage laws, Title 18, U.S.C., Secs. 793 and 794, the transmission or revelation of which in any manner to an unauthorized person is prohibited by law.

# NATIONAL AERONAUTICS AND SPACE ADMINISTRATION

WASHINGTON

May 1959

UNCLASSIFIED

AD 307 266

~~CONFIDENTIAL~~

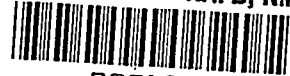
810 203301/246

2 cds removed 20 Jan 64 for

TECH LIBRARY

2 cds removed 20 Jan 64 fa

TECH LIBRARY KAFB, NM



0096276

1G

NATIONAL AERONAUTICS AND SPACE ADMINISTRATION

MEMORANDUM 5-6-59L

DAMPING IN PITCH AND STATIC STABILITY OF A GROUP OF  
BLUNT-NOSE AND CONE-CYLINDER-FLARE MODELS  
AT A MACH NUMBER OF 6.83\*

By Herman S. Fletcher and Walter D. Wolhart

SUMMARY

An investigation was made in the Langley 11-inch hypersonic tunnel at a Mach number of 6.83 and Reynolds number of approximately  $3.4 \times 10^6$  per foot to determine the damping in pitch and static stability of several cone-cylinder-flare and blunt-nose models using a free-oscillation technique. The test results indicated that the cone, blunted-cone-cylinder with flare, and blunt cylinder with flare were dynamically and statically stable and that the short blunt-nose models were dynamically unstable and statically stable. The generally poor agreement between measured and calculated (Newtonian impact theory) dynamic derivatives for configurations other than the cone is largely attributed to flow separation. Calculations for the blunted-cone-cylinder-flare body indicated that, if the shape and extent of the separated-flow region is known, the dynamic derivatives may be calculated fairly accurately by modifying the body to include the separated-flow region.

INTRODUCTION

Accurate estimates of the various aerodynamic parameters involved in the calculation of the motion of a ballistic missile are required if the motions are to be predicted with any degree of accuracy. Since there are no proven theoretical methods available for estimating all of these derivatives for the various geometries of interest, experimental methods must be utilized to acquire accurate values. However, relatively little of this experimental data is available for geometries of interest at present. (See refs. 1, 2, 3, 4, and 5.)

Therefore, tests in the hypersonic speed regime were initiated to provide damping-in-pitch and static-stability data on several blunt-nose and blunted-cone-cylinder-flare models. These last models are of a

\*Title, Unclassified.

SWC 908985/246

form suitable for supersonic impact ballistic-missile reentry bodies (ref. 6). The blunt-nose models tested possess desirable characteristics from heat-transfer considerations. (See ref. 7.) Some of these are of a form suitable for manned reentry capsules. Comparisons are also made between experiment and Newtonian impact theory (ref. 8). The tests were made in the Langley 11-inch hypersonic tunnel at a Mach number of 6.83.

## SYMBOLS

A	maximum cross-sectional area of model, sq ft	L
d	maximum diameter of model or maximum flare diameter for flared models, ft	2
K	spring constant, ft-lb/radian	3
I	moment of inertia in pitch, slug-ft <sup>2</sup>	8
P	period of oscillation, sec	
R	Reynolds number per foot	
t	time, sec	
$t_{1/2}$	time to damp to one-half amplitude, sec	
W	model weight, lb	
$q_0$	dynamic pressure, $\frac{\rho}{2} V^2$ , lb/sq ft	
q	pitching velocity, radians/sec	
V	velocity, ft/sec	
$\rho$	density, slugs/cu ft	
$\alpha$	angle of attack, deg	
$\dot{\alpha} = \partial\alpha/\partial t$		
$\omega$	circular frequency, radians/sec	
M	pitching moment about center of gravity, ft-lb	
$C_m$	pitching-moment coefficient, $M/q_0 A d$	

$C_{m\alpha}$  static-stability parameter,  $\partial C_m / \partial \alpha$ , per radian

$$C_{mq} = \frac{\partial C_m}{\partial \frac{q\dot{d}}{2V}}, \text{ per radian}$$

$$C_{m\dot{\alpha}} = \frac{\partial C_m}{\partial \frac{\dot{\alpha}d}{2V}}, \text{ per radian}$$

$C_{mq} + C_{m\dot{\alpha}}$  dynamic-stability parameter, per radian

## MODELS, INSTRUMENTATION, AND TESTS

### Models

Side-view drawings of the models (bodies of revolution) are shown in figure 1. Photographs of the models are shown in figure 2. Each model was machined from aluminum and in some cases, in order to aid balancing, partly of brass or an alloy of 97-percent tungsten and 3-percent copper. Each model was mass balanced so that the center of gravity corresponded to the pivot axis of the crossed-flexures strain gage. The static-stability and damping-in-pitch measurements are referred to the centers of gravity shown in figure 1.

### Instrumentation

The models were oscillated on a crossed-flexures strain gage (fig. 3); the signals of which were proportional to the model angular displacement in pitch. The recording equipment consisted of an oscillator and a consolidated recorder. The strain-gage signal was amplified by the carrier amplifier, demodulated, and then fed into the consolidated recorder. In the consolidated recorder, a spotlight galvanometer converted the electrical signal into an optical signal which was recorded on photographic paper. A photograph of the recording equipment is presented as figure 4.

### Tests

The tests of this investigation were made in the Langley 11-inch hypersonic tunnel at an average Mach number of 6.83 and a Reynolds number of approximately  $3.4 \times 10^6$  per foot. A description of this test facility may be found in reference 9. The reduced-frequency parameter  $\omega d / 2V$

varied from 0.0012 to 0.017, depending on the moment of inertia of each model. The test procedure consisted of plucking the model to a maximum amplitude of  $3.5^\circ$  and recording the resulting oscillation on photographic paper. All tests were made with the model oscillating about a mean angle of attack of  $0^\circ$ . The procedure of plucking the model and, in addition, holding it motionless during tunnel starting and stopping was accomplished by a mechanical linkage.

Three wind-on and wind-off records were taken for each model. A sample record for model 6 is shown as figure 5. The data shown in table I are the average  $C_{m_q} + C_{m_{\dot{\alpha}}}$  and  $C_{m_\alpha}$  values for the three runs. The average  $C_{m_q} + C_{m_{\dot{\alpha}}}$  value varied approximately 5 percent from the maximum or minimum value determined from each record. The period of the oscillation could be determined to within an estimated accuracy of 0.001 second. Thus, the maximum possible error in the calculation of the experimental  $C_{m_\alpha}$  is estimated to be 10 percent.

L  
2  
3  
8

#### REDUCTION OF DATA

The equations governing a single-degree-of-freedom free-oscillation system are given in reference 10 or any of several text books on mechanical vibrations (for example, ref. 11). The static-stability parameter  $C_{m_\alpha}$  and damping-in-pitch parameter  $C_{m_q} + C_{m_{\dot{\alpha}}}$  are given in terms of the frequency of motion and rate of damping by the following equations:

$$C_{m_\alpha} = - \frac{4\pi^2 I}{(P^2)_{\text{wind on}} q_0 Ad} + \frac{K}{q_0 Ad} \quad (1)$$

$$C_{m_q} + C_{m_{\dot{\alpha}}} = - \frac{2.772 IV}{q_0 Ad^2} \frac{1}{(t_{1/2})_{\text{aerodynamic}}} \quad (2)$$

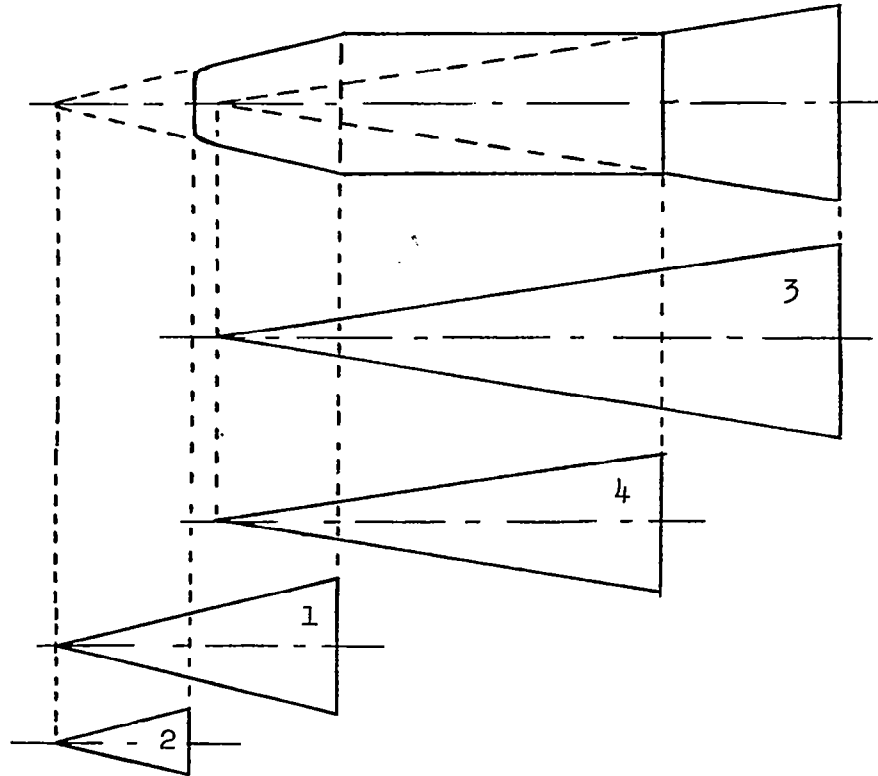
where  $I = (KP^2)_{\text{wind off}} / 4\pi^2$  and is obtained from the wind-off record. There was some variation of the spring constant  $K$  with axial load so that it was necessary to take this variation into account when computing  $C_{m_\alpha}$ .

Previous experience has shown the internal damping of the crossed flexures to be a function of amplitude but not of frequency. A data-reduction method was set up in which the internal damping was subtracted from each cycle of the wind-on record in accordance with this consideration. The amplitude of the oscillation corrected for internal damping was plotted against time on semilogarithmic paper and the time to damp to one-half amplitude read directly from the plots as  $(t_{1/2})_{\text{aerodynamic}}$ . These data were used in equations (1) and (2) to calculate the static stability and damping in pitch.

## RESULTS AND DISCUSSION

A comparison of experimental and calculated results for each model is shown in table I along with the Reynolds number per foot, dynamic pressure, weight, and moment of inertia for the particular test.

The dynamic and static stability were calculated using Newtonian impact theory (ref. 8). In these calculations, the Newtonian result was approximated by the addition and subtraction in an appropriate way of the Newtonian result for conical and spherical bodies. For example, it can be seen with the aid of the following sketch:



that

$$C_{m\alpha} = (C_{m\alpha})_1 - (C_{m\alpha})_2 + (C_{m\alpha})_3 - (C_{m\alpha})_4$$

$$C_{mq} = (C_{mq})_1 - (C_{mq})_2 + (C_{mq})_3 - (C_{mq})_4 + (C_{mq})_{\text{flat nose}}$$

The cylindrical portions of the body make no Newtonian contribution.

The theory of reference 8 does not give the contribution of the circular flat-plate nose to  $C_{mq}$ , but a value of  $C_{mq}$  of -0.5 based on the flat-plate diameter can be readily derived from elementary Newtonian considerations.

The experimental data showed each model to be statically stable (table I). Calculated values of  $C_{m\alpha}$  for the short blunt-nose models (models 1 and 2) and the cone (model 3) were in good agreement with experimental results, but calculated values of  $C_{m\alpha}$  for the extremely blunt body (model 5) were considerably smaller than the experimental values. The calculated values for the blunt-nose cylinder with flare (model 4) and the blunted-cone-cylinders with flare (models 6 and 7) considerably overestimated the level of static stability.

Models 3, 4, 6, and 7 were dynamically stable, but all other models were dynamically unstable. The dished nose of model 7 as compared with the flat nose of model 6 reduced the level of dynamic stability by a factor of 2. For models 3, 4, 6, and 7, the dynamic-stability values obtained from the theory of reference 8 had the same sign as the values obtained experimentally, but the quantitative agreement was poor, especially for models 6 and 7. For models 1, 2, and 5, Newtonian impact theory predicted values of opposite sign from experimental values.

It is apparent from the results of this investigation that, at least for the Mach and Reynolds number of these tests, measured dynamic derivatives are required for configurations appreciably different from a cone if the motions are to be predicted with any degree of accuracy. The generally poor agreement between measured and calculated dynamic derivatives for configurations other than the cone (model 3) is largely attributed to flow separation on the models. (See refs. 12, 13, 14, and 15.) In addition, the theory of reference 8 applies only to bodies having continually growing cross sections and is violated for portions of the bodies for models 1, 2, and 5.

Although the effects of Reynolds number were not included in the investigation, it is well known that Reynolds number may have an appreciable effect on the flow characteristics. It is interesting to note

that low-subsonic-speed tests of noncircular cylinders (ref. 16) have shown that the normal force is especially critical and very often undergoes a change in sign with a change in Reynolds number. Since the Reynolds numbers of these tests lie within the range where these force reversals occur ( $0.5 \times 10^6$ ), it is considered likely that the undamped motions of the short blunt models could be attributed to some extent to the possible reversal of normal force in this Reynolds number range. For cone-cylinder-flare bodies, the investigation reported in reference 12 indicated that at the Mach number and Reynolds number of this investigation there is a good possibility of laminar-boundary-layer separation occurring at the base of the nose cone and extending over an appreciable portion of the base flare. Reference 12 further shows that, if the body is modified to include this separated-flow region, considerably better agreement is obtained between measured and calculated values of normal-force-curve slope and center of pressure. Based on this result, an attempt was made to account for the effects of separation on the damping in pitch and static stability of a cone-cylinder-flare body by modifying the shape to include the separated-flow region. Calculations for model 6 on which the separated-flow region was estimated to extend from the base of the nose cone to the base of the flare yielded values of  $C_{mq}$  and  $C_{m\alpha}$  of -2.23 and -0.32, respectively, which are in better agreement with measured values than the values calculated neglecting separation. Although the noses of models 4 and 7 are appreciably different from the nose of model 6, it was assumed that the flow separated in the same manner as on model 6. Calculations for these modified bodies yielded values of  $C_{mq}$  and  $C_{m\alpha}$  of -1.10 and -0.30, respectively, for model 4 and -2.24 and -0.40 for model 7. These values are in better agreement with measured values for  $C_{m\alpha}$  than the unseparated-flow values but showed poorer agreement for  $C_{mq}$ .

These attempts to account for the effects of separated flow on the aerodynamic characteristics of cone-cylinder-flare bodies by modifying the shape to include the separated-flow region indicate that fairly good estimates of the aerodynamic derivatives can be made if information is available on the extent and shape of the separated-flow regions. It also indicated, as might be expected, that while the information on the separated-flow region does not have to be for a body identical to the proposed body the more nearly the proposed body is to that for which information is available, the more reliable the calculated derivatives will be.



## CONCLUSIONS

The results of an investigation to determine the static stability and damping in pitch of several blunt-nose and cone-cylinder-flare models at Mach 6.83 using a free-oscillation technique indicate the following conclusions:

1. All models were statically stable.
2. The short blunt-nose models were dynamically unstable and the flared cylinder models were dynamically stable.
3. The generally poor agreement between measured and calculated dynamic derivatives for configurations other than a cone is largely attributed to flow separation.
4. Calculations for the cone-cylinder-flare body indicated that if the shape and extent of the separated-flow region is known fairly good estimates of the damping in pitch and static stability may be made by modifying the body to include the separated-flow region.



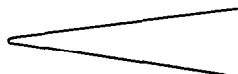

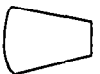
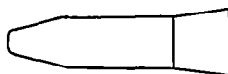
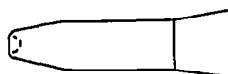
Langley Research Center,  
National Aeronautics and Space Administration,  
Langley Field, Va., February 12, 1959.

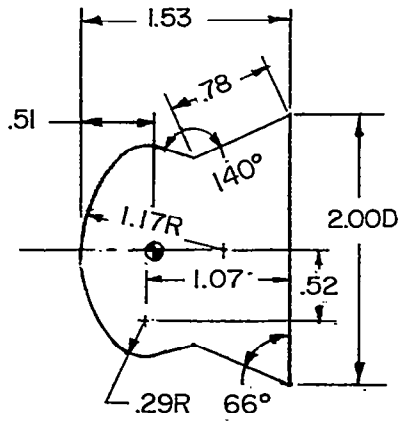
## REFERENCES

1. Kehlet, Alan B.: Some Effects of Reynolds Number on the Stability of a Series of Flared-Body and Blunted-Cone Models at Mach Numbers From 1.62 to 6.86. NACA RM L57J29, 1957.
2. Bird, John D., and Reese, David E., Jr.: Stability of Ballistic Reentry Bodies. NACA RM L58E02a, 1958.
3. Coltrane, Lucille C.: Stability Investigation of a Blunt Cone and a Blunt Cylinder With a Square Base at Mach Numbers From 0.64 to 2.14. NACA RM L58G24, 1958.
4. Tom, William S.: Aerodynamic Characteristics of the ML-404-20 Polaris Re-Entry Models; Preliminary Results. Tech. Note 5034-32, U. S. Naval Ord. Test Station (China Lake, Calif.), Nov. 14, 1957.
5. Fenske, J. F.: Preliminary Results of Dynamic Stability Tests in the AEDC E-1 Supersonic Wind Tunnel. RAD Tech. Memo 2-TM-57-61 (Aerod. Sec. Memo No. 146), AVCO Res. and Advanced Dev. Div., Aug. 26, 1957.
6. Hall, James R., and Garland, Benjamine J.: A Feasibility Study of the Flare-Cylinder Configuration as a Reentry Body Shape for an Intermediate Range Ballistic Missile. NACA RM L58C21, 1958.
7. Allen, H. Julian, and Eggers, A. J., Jr.: A Study of the Motion and Aerodynamic Heating of Missiles Entering the Earth's Atmosphere at High Supersonic Speed. NACA TN 4047, 1957. (Supersedes NACA RM A53D28.)
8. Tobak, Murray, and Wehrend, William R.: Stability Derivatives of Cones at Supersonic Speeds. NACA TN 3788, 1956.
9. McLellan, Charles H., Williams, Thomas W., and Beckwith, Ivan E.: Investigation of the Flow Through a Single-Stage Two-Dimensional Nozzle in the Langley 11-Inch Hypersonic Tunnel. NACA TN 2223, 1950.
10. Campbell, John P., and Mathews, Ward O.: Experimental Determination of the Yawing Moment Due to Yawing Contributed by the Wing, Fuselage, and Vertical Tail of a Midwing Airplane Model. NACA WRL-387, 1943. (Formerly NACA ARR 3F28.)
11. Den Hartog, J. P.: Mechanical Vibrations. Fourth ed., McGraw-Hill Book Co., Inc., 1956.

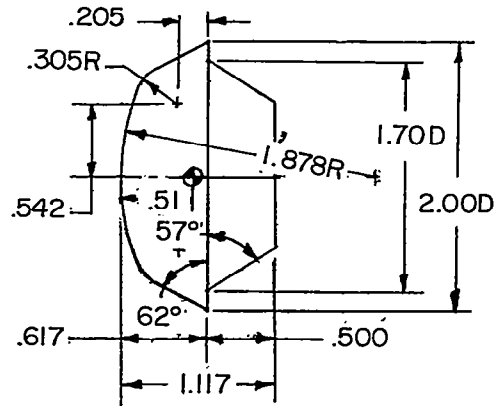
12. Dennis, David H.: The Effects of Boundary-Layer Separation Over Bodies of Revolution With Conical Tail Flares. NACA RM A57I30, 1957.
13. Eggers, A. J., Jr., and Syvertson, Clarence A.: Experimental Investigation of a Body Flare for Obtaining Pitch Stability and a Body Flap for Obtaining Pitch Control in Hypersonic Flight. NACA RM A54J13, 1955.
14. Becker, John V., and Korycinski, Peter F.: Heat Transfer and Pressure Distribution at a Mach Number of 6.8 on Bodies With Conical Flares and Extensive Flow Separation. NACA RM L56F22, 1956.
15. Canning, Thomas N., and Sommer, Simon C.: Investigation of Boundary-Layer Transition on Flat-Faced Bodies of Revolution at High Supersonic Speeds. NACA RM A57C25, 1957.
16. Polhamus, Edward C.: Effect of Flow Incidence and Reynolds Number on Low-Speed Aerodynamic Characteristics of Several Noncircular Cylinders With Applications to Directional Stability and Spinning. NACA TN 4176, 1958.

TABLE I.- EXPERIMENTAL AND CALCULATED RESULTS, TEST CONDITIONS, AND MASS CHARACTERISTICS OF MODELS

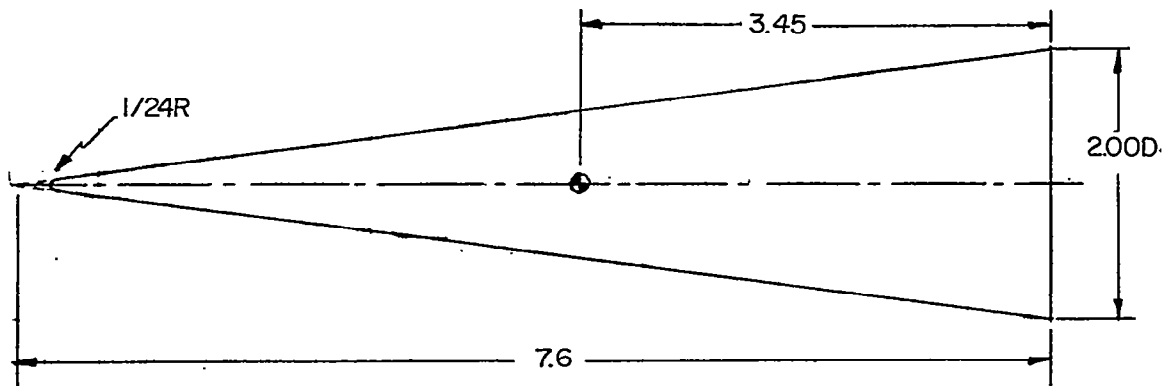
Model	Sketches	$C_{m_q} + C_{m_{\dot{\alpha}}}$	$C_{m_{\alpha}}$	Calculated $C_{m_q}$	Calculated $C_{m_{\alpha}}$	R per foot	$q_0$ , lb/sq ft	W, lb	$I$ , slug-ft <sup>2</sup>
1		0.29	-0.41	-0.32	-0.39	$3.233 \times 10^6$	472.2	0.164	0.00001579
2		0.28	-0.21	-0.23	-0.24	3.357	468.8	0.146	0.00000959
3		-2.80	-1.05	-4.30	-1.00	3.438	479.7	0.336	0.0003609
4		-4.06	-0.05	-2.64	-1.05	3.363	467.6	0.343	0.0002518
5		0.37	-0.45	-0.33	-0.14	3.312	482.0	0.304	0.0000404
6		-1.96	-0.17	-6.47	-0.80	3.358	462.2	0.401	0.0003104
7		-0.83	-0.27	-5.98	-0.98	3.417	464.6	0.409	0.0003272



(a) Model 1.



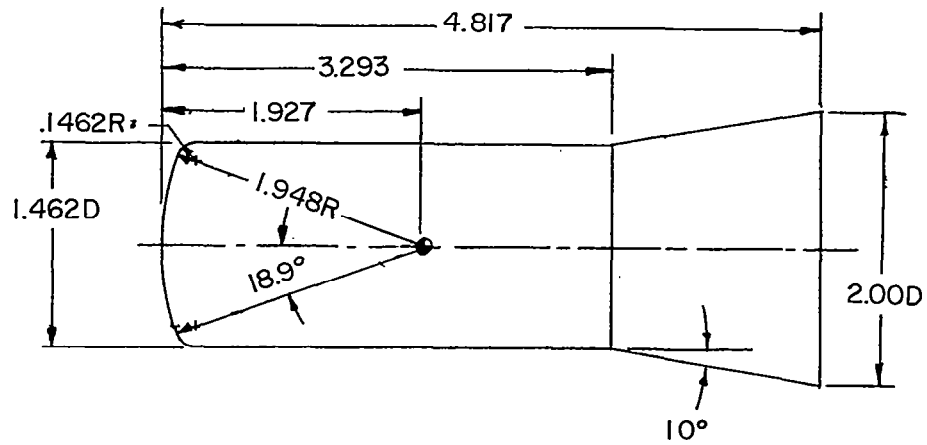
(b) Model 2.



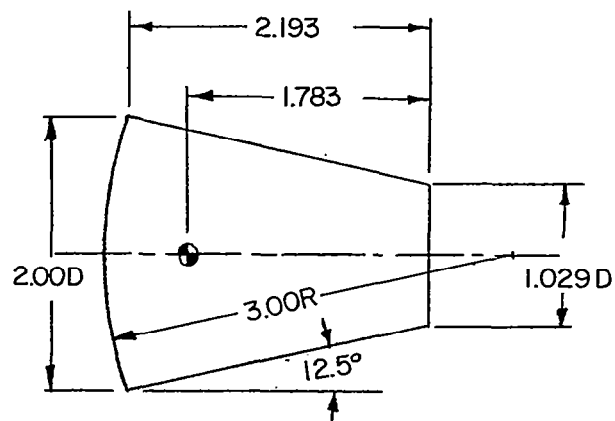
(c) Model 3.

Figure 1.- Drawing of models. All dimensions are in inches.

L-238

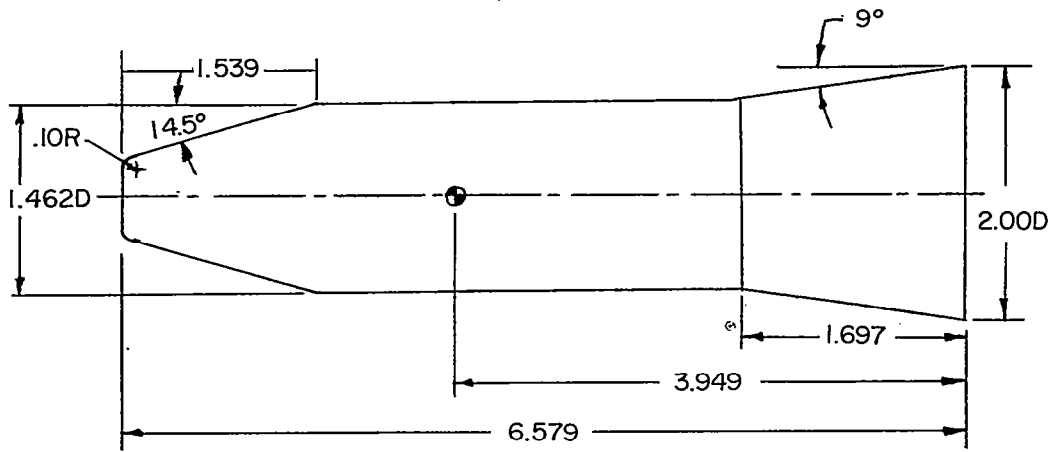


(d) Model 4.

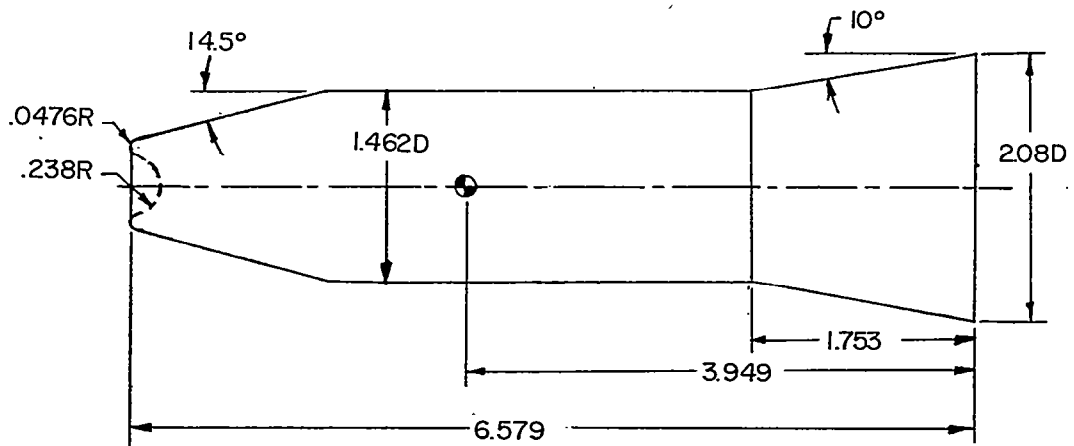


(e) Model 5.

Figure 1.- Continued.



(f) Model 6.



(g) Model 7.

Figure 1.- Concluded.

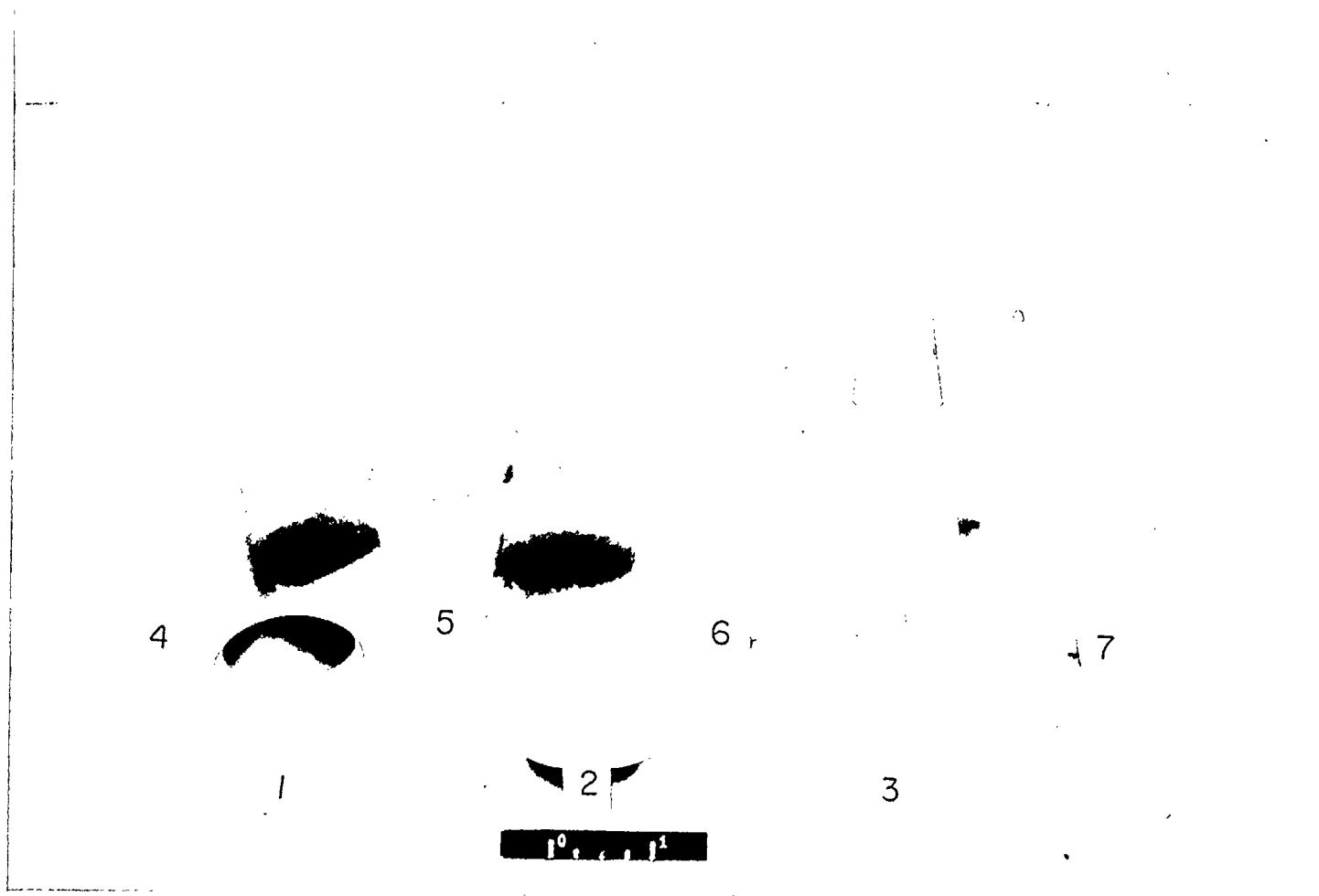


Figure 2.- Photographs of models. L-58-3634.1



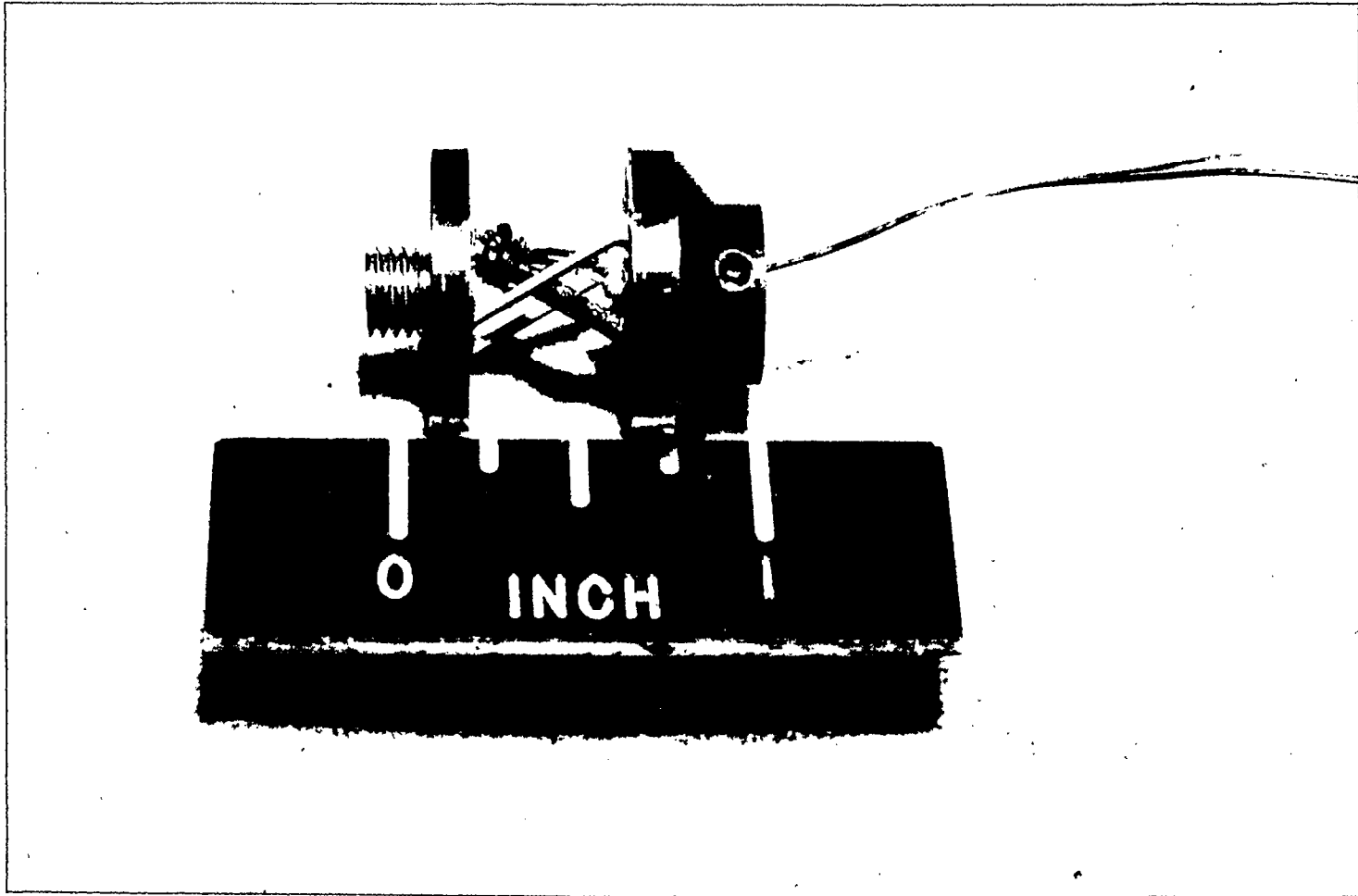


Figure 3.- Photograph of crossed-flexures strain gage. L-58-1578

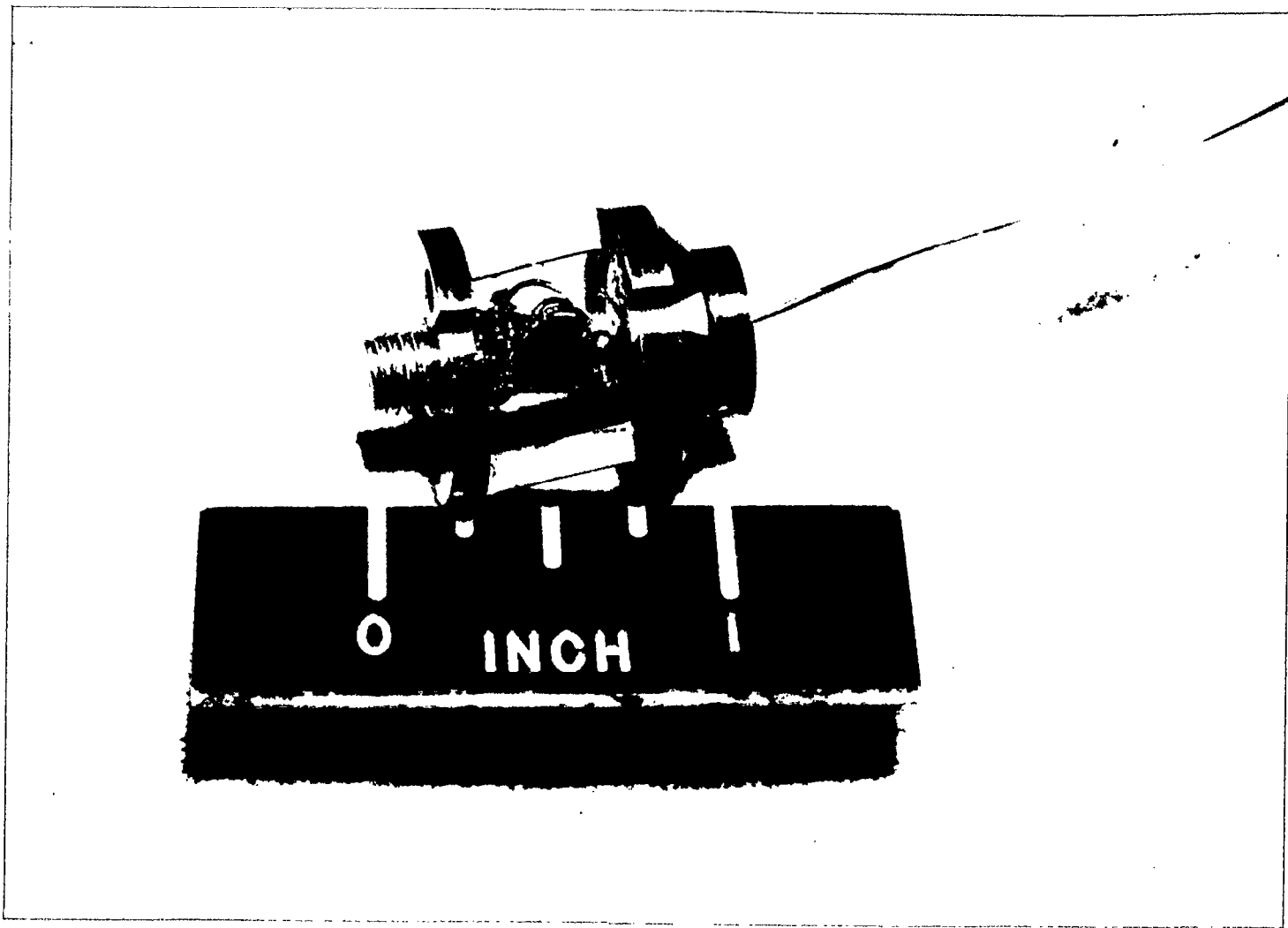


Figure 3.- Concluded.

L-58-1579

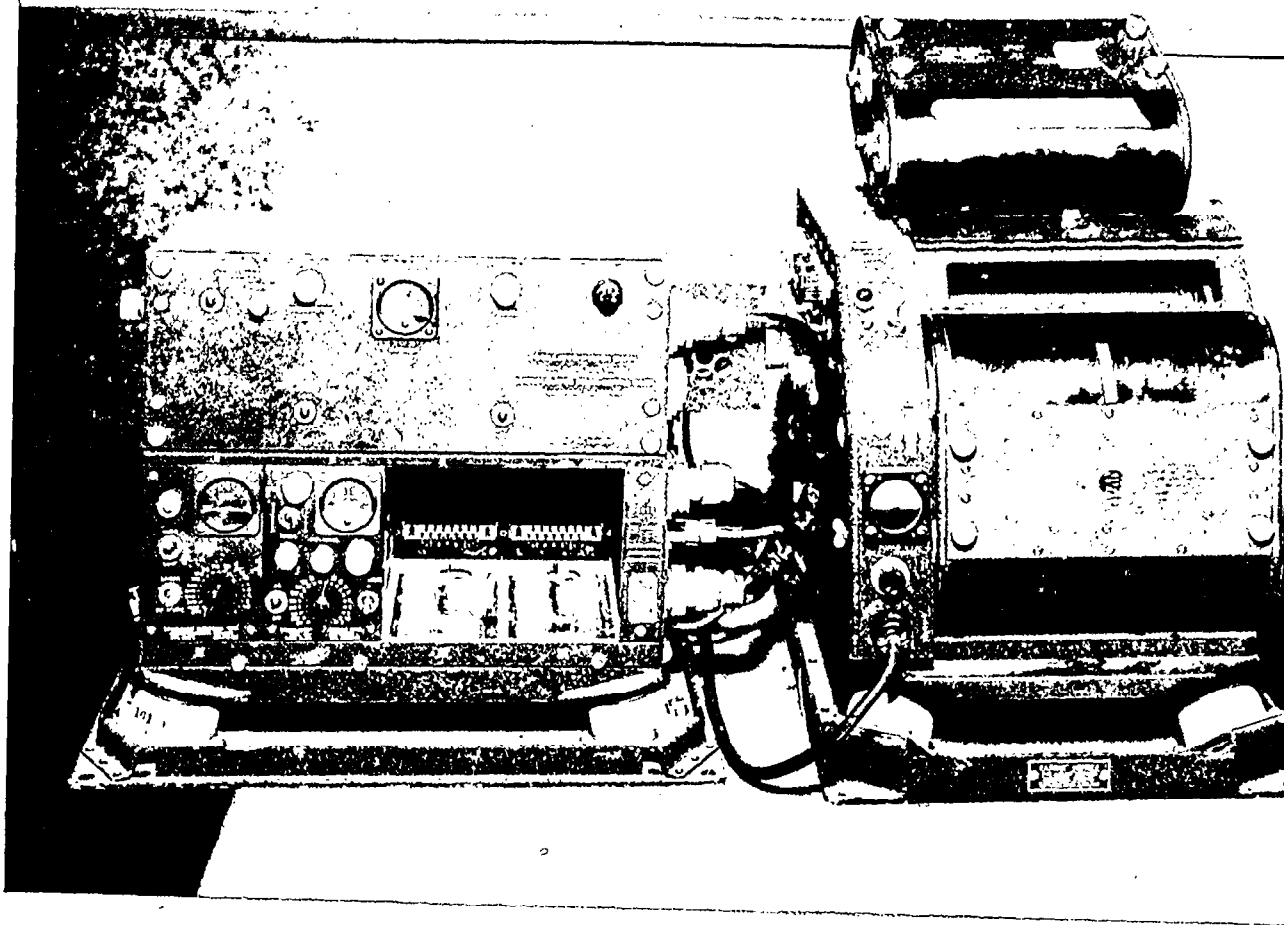


Figure 4.- Photograph of recording equipment. L-58-964.1

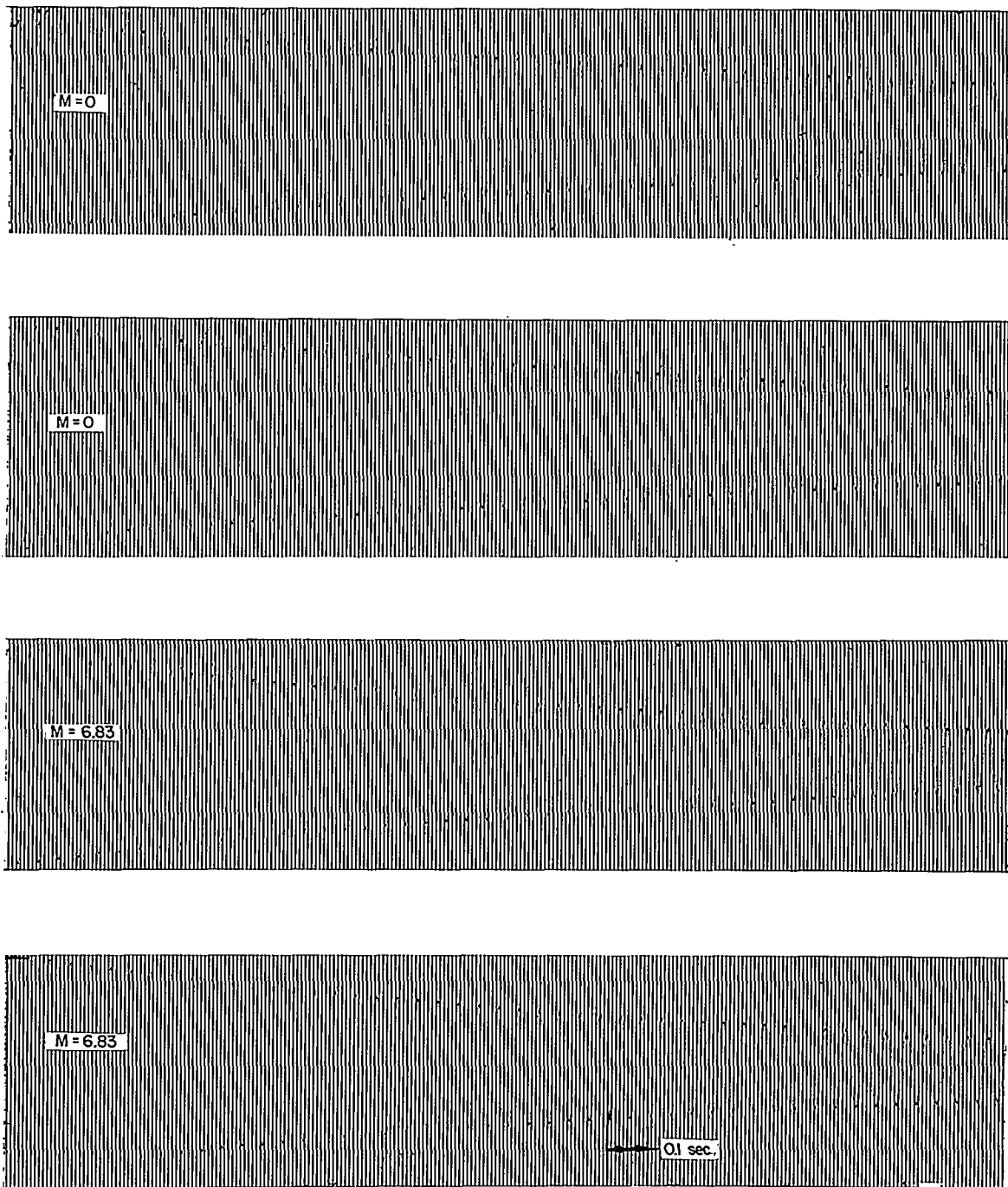


Figure 5.- Typical oscillation records for model 6.